

## ONE-, TWO-, AND THREE-DIMENSIONAL NUMERICAL SIMULATION OF TWO-BEAM PLASMAS\*

R. L. Morse and C. W. Nielson

University of California, Los Alamos Scientific Laboratory, Los Alamos, New Mexico 87544

(Received 25 September 1969)

Comparable one-, two-, and three-dimensional simulations of electrostatic two-beam instabilities show major qualitative differences between one and two dimensions, and only small quantitative differences between two and three dimensions. In particular, the well-known persistence of vortex structure is lost in going from one dimension to two and three dimensions.

This paper presents results of comparable one-, two-, and three-dimensional numerical simulations of electrostatic two-beam instabilities in collisionless plasma. In all cases the ions are treated as a uniform, fixed, positive background, and the initial electron distribution is spatially uniform with a velocity distribution consisting of two drifting Maxwellian beams:

$$f_0(\vec{v}) = \frac{n_1}{\pi^{3/2}v_1^3} e^{-(\vec{v}-u_1\hat{x})^2/v_1^2} + \frac{n_2}{\pi^{3/2}v_2^3} e^{-(\vec{v}-u_2\hat{x})^2/v_2^2}. \quad (1)$$

No generality is lost by taking the  $x$  axis parallel to the drift velocities,  $u_1$  and  $u_2$ . Combinations of the densities  $n_1$  and  $n_2$ , the thermal spreads  $v_1$  and  $v_2$ , and the drift velocities  $u_1$  and  $u_2$  which make the two beams of  $f_0$  sufficiently distinct, are known from linear theory to support unstable growth of electrostatic waves for which the perturbed potential has the form

$$\varphi \sim \exp(i(\vec{k} \cdot \vec{x} - \omega t)). \quad (2)$$

When such modes are unstable the largest growth rates, i.e., values of  $\text{Im}\omega$ , belong to modes with pure  $k_x$ . The growth rates are largest for intermediate values of  $k$ , and fall to zero for  $k \rightarrow 0$  and above a finite cutoff value of  $k$ . The one-dimensional problem has received a lot of study including, recently, some full nonlinear simulations.<sup>1-4</sup> A one-dimensional (1-d) treatment may be justified because of its simplicity, the fact that the fastest growing modes develop in the restricted  $(x, v_x)$  one-dimensional problem, and also because of a limited class of experiments for which the 1-d description is sufficient. Some of the results of these 1-d simulations, including strong, persistent single-mode structure, seem to conflict with basic assumptions of plasma turbulence theory,<sup>5,6</sup> but it has also been widely suspected that these 1-d results are dominated by the symmetry of the restriction to  $x$  dependence. This paper extends the work of Refs. 3

and 4 to two and three dimensions in such a way that the transition from one dimension can be clearly seen.

A particular three-dimensional  $f_0(v_x, v_y, v_z)$ , Eq. (1), and a particular periodicity length  $L$  are chosen. The three-dimensional simulation is done in a cube of length  $L$  with periodic boundary conditions on the electron motion and the electrostatic potential  $\varphi(x, y, z)$ , and starting with the spatially uniform electron distribution  $f_0$ . The two-dimensional simulation is done in an  $(x, y)$  square of length  $L$  with periodic boundary conditions, and starting with the  $f_0(v_x, v_y)$  velocity distribution obtained by integrating Eq. (1) over  $v_z$ . The one-dimensional simulation is done in  $x$  alone with a periodicity length  $L$  and the  $f_0(v_x)$  distribution obtained by integrating Eq. (1) over  $v_y$  and  $v_z$ .

The electrons are treated by the particle-in-cell method which is described in more detail in Refs. 3 and 4. The one-, two-, or three-dimensional region is divided regularly into Eulerian cells for the purpose of solving Poisson's equation for  $\varphi$  and interpolating the resulting fields. The electrons are represented by simulation particles which follow electron trajectories, but in general represent many electrons each. On each computational time step, cell-center charges are computed by apportioning each particle's charge through a linear weighting to the nearest-neighbor cell centers (two, four, or eight neighbors, depending on dimensionality). Poisson's equation is solved on the grid of cell centers, the resulting  $E$  field is interpolated to individual particle positions, and the particles' velocities and positions are advanced by time-centered differences.

Figure 1 shows (a) an initial  $(x, v_x)$  phase-space plot of a random subset of simulation particles and (b)  $f_0(v_x)$  for the two equal-warm-beam distributions  $u_1 = -u_2 = 2v_1 = 2v_2$ , with  $L = 100$  Debye lengths. Figure 2 shows diagnostics from (a) 1-d, (b) 2-d, and (c) 3-d comparison runs of this case whose one-dimensional behavior is reported

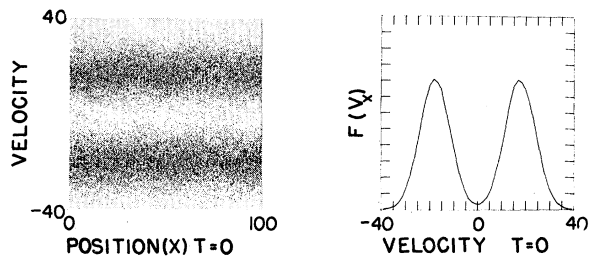


FIG. 1. Initial conditions for two equal counterstreaming beams.

in Refs. 3 and 4 with greater  $L$ , showing formation, coalescing, and long-time persistence of Bernstein, Green, and Kruskal (B.G.K.) modes<sup>7</sup> as seen here in Fig. 2. The initial perturbations in all runs are introduced by the random numbers used, in conjunction with a mapping function in the velocity initialization as described in Refs. 3 and 4. Each column in Fig. 2 shows two  $(x, v_x)$  phase plots, the first at field-energy-saturation time and the second at the final time of 10 plasma periods,  $T_p = 2\pi\omega_p^{-1}$ , followed by

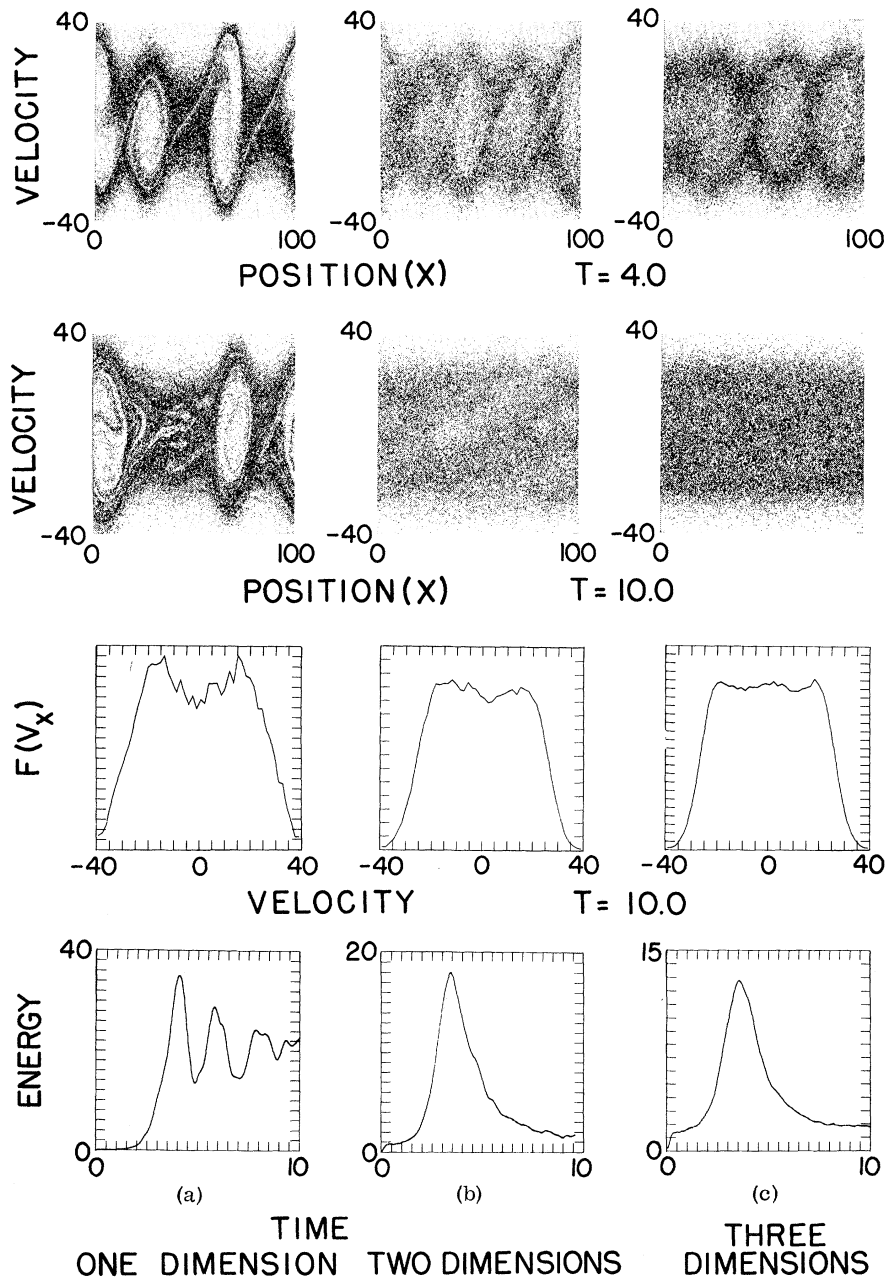


FIG. 2. Results of two equal beam simulations in one, two, and three dimensions.

$f(v_x)$  at final time and the time history,  $\mathcal{E}(t)$ , of the total electrostatic-field energy per unit volume. In all three runs the field energy first rises to the thermal level and then rises unstably until saturation, at first exponentially at the rate of the fastest linear mode and with most of the field energy in the corresponding  $|E_{\vec{k}}|^2$ . (Fourier mode-energy plots were computed but are not shown here.) This concentration of energy in the fastest-growing modes is a natural consequence of growing a few  $e$ -folding times from a low, uniform, initial noise spectrum.<sup>4</sup> Extensive error checks which have been performed<sup>3,4</sup> indicate that the number of simulation particles must be great enough to reduce the initial thermal level far below the maximum or saturation level of  $\mathcal{E}(t)$ . When this condition is fulfilled, most of the field energy appears in the  $|E_{\vec{k}}|^2$ 's corresponding to those modes of intermediate wavelength with the largest growth rates, in contrast to the  $1/k^2$  thermal noise spectrum. If these criteria are not satisfied, the correct collisionless results are not simply superposed on the thermal noise level but are instead destroyed by the noise. The height of the early thermal  $\mathcal{E}(t)$  plateau increases in going from one to three dimensions here because restrictions on computer time and memory precluded increasing the number of simulation particles in going to two and three dimensions by enough to retain the low noise level of the 1-d run: The 1-d run used 20 000 particles which was more than enough; the 2-d run used 80 000; and the 3-d run used 332 750, which was just barely adequate. The number of simulation particles required from noise considerations could be reduced by reducing  $L$  below 100 Debye lengths but then the number of modes would be unduly restricted. A time step of 0.04 plasma periods was used here, as in Refs. 3 and 4, for the reasons given in the error analysis there.

The most obvious physical change occurs between 1-d and 2-d. In 1-d the phase-space eddies coalesce until one eddy remains in the length  $L$ , and  $\mathcal{E}$  decreases after the overshoot to a level consistent with this stationary structure. If  $L$  is greater, further coalescing occurs and  $\mathcal{E}$  levels off at a correspondingly lower value, but one eddy remains and  $\mathcal{E}$  does not go back down to the thermal level. In 2-d the eddies start to form, as seen in Fig. 2, at saturation time, but do not form completely and have virtually disappeared by the final time. Correspondingly,  $\mathcal{E}(t)$  saturates at a lower level in 2-d than in 1-d (note the

scale changes on the plots) and then falls quickly to about the initial thermal level. In 3-d these changes from 1-d become more pronounced. The partially formed eddies are less distinct than in 2-d, and the saturation value of  $\mathcal{E}$  is still lower. The simulation particles shown in the  $(x, v_x)$  phase plots for 2-d and 3-d are taken from a slab restricted in  $y$  to reduce the effect of finite  $k_y$  modes in blurring the appearance of the eddies.

The final-time  $f(v_x)$  plots in Fig. 2, which are generated by a simple histogram procedure without any smoothing, are smoother for the higher-dimensional runs because of the improved statistics. All three  $f(v_x)$  curves are plotted on the same velocity scale of  $[-40, 40]$  Debye lengths per plasma period and show that the 2-d and 3-d curves are essentially unchanged from  $f_0(v_x)$  in the tails, i.e., outside  $[-30, 30]$ , while in 1-d the tails are somewhat broadened by the persistent, large-amplitude eddy structure. This same eddy structure gives the final-time 1-d  $f(v_x)$  a definite dip in the middle, while in the higher-dimensional runs, which are spatially uniform by this time,  $f(v_x)$  is essentially flat on top, especially in 3-d. That the middle of the electron distribution should become quite flat as a result of multi-dimensional strong turbulence may be related to similar experimental findings from satellites in the shocked region behind the earth's bow shock.<sup>8</sup>

A beam-and-cool-background case,  $u_1 = 0$ ,  $n_2 = n_1/20$ ,  $v_2 = v_1$ , and  $u_2 = 10.5v_1$ , was treated in Refs. 3 and 4 in 1-d and showed a rapid spreading of the beam,  $n_2$ , by about  $\pm u_2$  with only incomplete formation of eddies. There a major fraction of the saturation  $\mathcal{E}$  remains in persistent undamped plasma oscillations of the cold background. In 2-d and 3-d, with  $L = 400$  Debye lengths (of the background), this case shows only moderate quantitative changes from 1-d except that after saturation the background oscillations damp out and  $\mathcal{E}(t)$  rapidly returns to thermal. In order to reduce fluctuations to an acceptable level for this case in 3-d, it was necessary to use 646 893 simulation particles.

A strong "bump-on-tail" case,  $u_1 = 0$ ,  $n_2 = n_1/20$ ,  $v_2 = 0.25v_1$ , and  $u_2 = 2.616v_1$ , was also run in Refs. 3 and 4 in 1-d and showed clear formation of eddies in the unstable part of phase space, but without coalescing, as well as flattening of the "bump on the tail" of  $f(v_x)$ , and a slowly decreasing superthermal level of  $\mathcal{E}(t)$  after the initial overshoot. The 2-d version of this case has now been done, but computer limitations have precluded the 3-d version. In 2-d,  $\mathcal{E}(t)$  falls to ther-

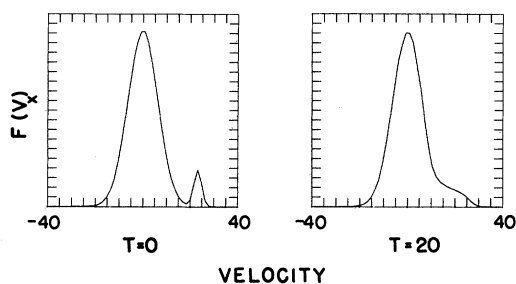


FIG. 3. Initial- and final-velocity distributions for strong "bump on tail" in two dimensions.

mal after saturation, much like the 2-d and 3-d curves in Fig. 2. Figure 3 shows  $f(v_x)$  at initial time and after 20 plasma periods, at which time  $\mathcal{E}(t)$  is back down to thermal, and  $f(v_x)$  appears to be stationary. This run used 379 600 simulation particles and  $L = 100$  Debye lengths. The evolution of the bump into a region of everywhere distinctly negative slope, in contrast to the simple flattening seen in 1-d, is consistent with the

theory of Bernstein and Engelmann.<sup>9</sup>

\*Work performed under the auspices of the U. S. Atomic Energy Commission.

<sup>1</sup>T. P. Armstrong and D. Montgomery, *J. Plasma Phys.* **1**, 425 (1967).

<sup>2</sup>K. V. Roberts and H. L. Berk, *Phys. Rev. Letters* **19**, 297 (1967).

<sup>3</sup>R. L. Morse and C. W. Nielson, *Bull. Am. Phys. Soc.* **13**, 1744 (1968).

<sup>4</sup>R. L. Morse and C. W. Nielson, "Numerical Simulation of Warm Two Beam Plasma" (to be published).

<sup>5</sup>W. E. Drummond and D. Pines, *Nucl. Fusion: Suppl.* Pt. 3, 1049 (1962).

<sup>6</sup>R. Z. Sagdeev and A. A. Galeev, in *Nonlinear Plasma Theory*, edited by T. M. O'Neil and D. L. Book (W. A. Benjamin, Inc., New York, 1969).

<sup>7</sup>I. B. Bernstein, J. M. Green, and M. D. Kruskal, *Phys. Rev.* **108**, 546 (1957).

<sup>8</sup>M. Montgomery, "Plasma Measurements Near the Earth's Bow Shock-Vela IV" (to be published).

<sup>9</sup>I. Bernstein and F. Engelmann, *Phys. Fluids* **9**, 937 (1966).

#### TRAPPING OF NEGATIVE IONS IN TURBULENT SUPERFLUID HELIUM\*

Donald M. Sitton

Department of Aerospace Engineering and Engineering Physics,  
University of Virginia, Charlottesville, Virginia 22901

and

Frank Moss

Research Laboratories for the Engineering Sciences, and  
Department of Aerospace Engineering and Engineering Physics,  
University of Virginia, Charlottesville, Virginia 22901

(Received 8 October 1969)

Capture and escape of negative ions by vorticity resulting from a supercritical heat current in liquid He II are demonstrated in the temperature range between 1.6 and 1.8°K. The vorticity is identical to that produced by rotation except for configuration of the individual lines. The escape probability was measured between 1.7 and 1.8°K and is in agreement with the theory of Donnelly.

Following its discovery by Careri, McCormick, and Scaramuzzi,<sup>1</sup> the ion-vortex-line interaction in liquid He II has received a great deal of attention. It has been shown that below 1.7°K, negative ions are captured by vortex lines<sup>2</sup> in a potential well created by the quantized circulation around the vortex axis, and that the ions escape by a thermal activation process,<sup>3,4</sup> at least in the range  $1.6 < T \leq 1.7^\circ\text{K}$ .<sup>5</sup> The escape probability  $P$ , the capture width  $\sigma$ , and the mobility along the lines have been extensively studied for ions captured on linear vortex arrays produced by rotation.<sup>6-9</sup> These well-established results have mo-

tivated us to study the structure of turbulent, bulk He II in the presence of a supercritical heat current using negative ions as probe particles. Previous experiments have indicated that ions interact strongly with the turbulence,<sup>10,11</sup> however no quantitative data on the interaction or turbulent structure have been obtained.

Our results indicate that (1) negative ions are captured by vortex lines produced by a supercritical heat current up to above 1.8°K; (2) the turbulent structure can be described as an irregular array, or "tangled mass" of vorticity as suggested by Vinen<sup>12</sup> and Hall<sup>13</sup>; and (3) the in-

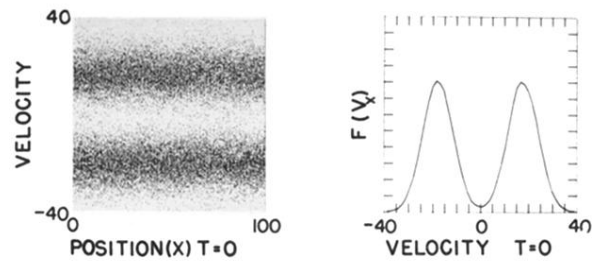


FIG. 1. Initial conditions for two equal counterstreaming beams.

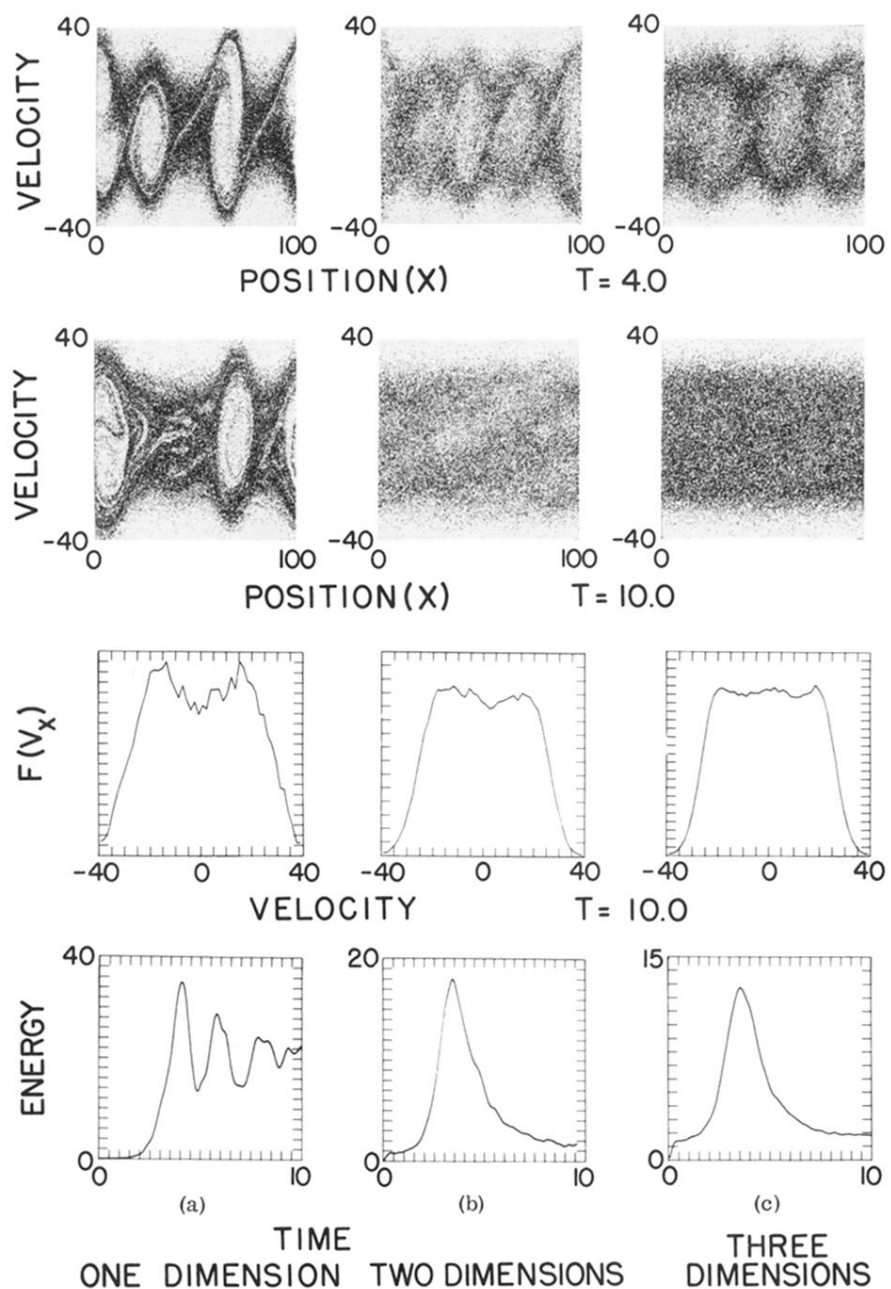


FIG. 2. Results of two equal beam simulations in one, two, and three dimensions.